

## Analysis of Dielectric Relaxation Spectra by Diffusive representations method : Case of Organic Dielectrics

**Abstract.** This paper deals with the phenomena of polarization and dielectric relaxation of organic dielectrics in the particular context of simulation and identification, the concept of diffusive representation was introduced in order to transform certain non-standard causal convolution operators such as fractional order integrations or derivations into dissipative input/output linear dynamic systems in a functional state space. The application of diffusive representations for the identification of the relaxation parameters of an organic dielectric has shown the efficiency of this method compared to others used in the field, particularly in terms of simulation time and working memory. The elaboration of behavioral state models of linear but non-rational input-output systems using diffusive representation has given, so the identification of the characteristic parameters of these models, gathered in the diffusive symbol, has also presented in the frequency and time domain. The parameter of discretization  $K$  has a significant effect on the results obtained, hence its delicate choice. The parameters of the Cole-Cole relaxation model were identified with acceptable precision, which opens a wide field of application of this method in applications of electrical engineering.

**Streszczenie.** W artykule omówiono zjawiska polaryzacji i relaksacji dielektrycznej dielektryków organicznych w szczególnym kontekście symulacji i identyfikacji. Pojęcie reprezentacji dyfuzyjnej zostało wprowadzone w celu przekształcenia niektórych niestandardowych operatorów spłotów przyczynowych, takich jak całki ułamkowe lub pochodne na dyssypatywne liniowe układy dynamiczne wejścia / wyjścia w funkcjonalnej przestrzeni stanów. Zastosowanie reprezentacji dyfuzyjnych do identyfikacji parametrów relaksacji organicznego dielektryka wykazało skuteczność tej metody w porównaniu z innymi stosowanymi w tej dziedzinie, szczególnie pod względem czasu symulacji i pamięci roboczej. Dano opracowanie behawioralnych modeli stanu liniowych, ale nieracjonalnych systemów wejścia-wyjścia z wykorzystaniem reprezentacji dyfuzyjnej, więc identyfikacja charakterystycznych parametrów tych modeli, zebranych w symbolu dyfuzyjnym, została również przedstawiona w dziedzinie częstotliwości i czasu. Parametr dyskretyzacji  $K$  ma istotny wpływ na uzyskiwane wyniki, stąd jego delikatny dobór. Parametry modelu relaksacji Cole-Cole'a zidentyfikowano z dopuszczalną precyzją, co otwiera szerokie pole zastosowań tej metody w zastosowaniach elektrotechniki. (*Analiza widm relaksacji dielektrycznej metodą reprezentacji dyfuzyjnych : Przypadek dielektryków organicznych*)

**Keywords:** dielectric relaxation, diffusive representation, Cole-Cole relaxation model, parameter of discretization

**Słowa kluczowe:** relaksacja dielektryczna, reprezentacja dyfuzyjna, model relaksacji Cole-Cole'a, parametr dyskretyzacji

### Introduction

The dielectrics properties of organic insulators are widely used in electrical engineering for applications such as cable connections, capacitors, coating of components, various supports. However, the electrical properties of these materials depend on the chemical structure of the macromolecules that make them up, but also on various factors and in particular on voluntary or involuntary excipients. The non-conductivity of insulating polymers makes it easy to observe a whole range of finer electrical effects. The consequent polarization of the distortion and the alignment of molecules under the influence of an applied field appear, for example. A dielectric material consists of atoms or molecules that possess one or more of the basic types of electrical polarization: [1-6] electronic, atomic or ionic, dipolar, spontaneous and interfacial polarization (or space charge). The phenomenon of polarization generally comes from the orientation of an electric dipole, induced or permanent, in the presence of an applied field, it corresponds to changes in the distribution of the bonded charges that make up the stable groups of matter (atoms, molecules, ions). Each type of polarization requires a time of realization, that is why the polarization of the whole depends on the temporal variation of the electric field.

The review of the literature has shown us the diversity of approaches used to study a rather complicated phenomenon such as dielectric relaxation, given that it has two aspects, microscopic and macroscopic on the one hand and its dependence on several factors such as temperature, frequency, the state of the material itself on the other hand. [1],[5],[ 7-9]. The electron and atomic polarizations are essentially due to the elastic displacements of electron clouds and vibrations in the network of atoms or molecules. Orientation polarization is a rotational process, which not only meets resistance due to thermal agitation, but also due to the inertial resistance of the surrounding molecules,

giving rise to mechanical friction. By virtue of an external force, it tends to change from its initial state of equilibrium to a new state of dynamic equilibrium, and when the force is removed, it relaxes and then returns to its initial state of equilibrium (relaxation process).

The numerical simulation of these phenomena, with classical methods, requires very complicated calculations, and therefore computers with an enormous capacity, so the search for new methods to reduce the cost of these calculations. Progress in the production of highly advanced measuring instruments, on the one hand, and the connection to computer equipment, which is equipped with ever-faster algorithms and optimization methods, has, on the other hand, made it possible to characterize these materials. In addition, analyze its characteristic variables with increased accuracy. However, in these field phenomena have known as 'long memory' such as relaxation of dielectric, this process requires enormous computation time and huge working memory, unacceptable things today, precisely in the field of research and simulation.

In 1998, G. Montseny and *a/* developed a new method called Diffuse Representation (DR), a mathematical tool that allows us to deal with objects with dynamic behavior with memory, folded, non-rational, and which can also include non-linearities. The ability to obtain accurate and compact models makes it an optional tool for modeling such objects.

This work will present the DR tool, its application in simulation, these different stages of development and its application in frequency and time identification. The use of this tool to identify a dielectric relaxation model of organic materials is the subject of this report. Our objective is to apply this method to the identification of the Cole-Cole relaxation model for organic dielectrics

## Relaxation Models

Fig.1 shows different effects on permittivity and dielectric loss of relaxation and resonance modes. We can see that a variation of the real permittivity causes a peak in the dielectric losses. In this figure, we find that the permittivity at frequencies higher than the optical frequencies is equal to 1 (vacuum contribution). Then, according to the decreasing frequencies: electronic and atomic polarizations which are resonance phenomena and dipole polarizations and space charge which are relaxation phenomena.

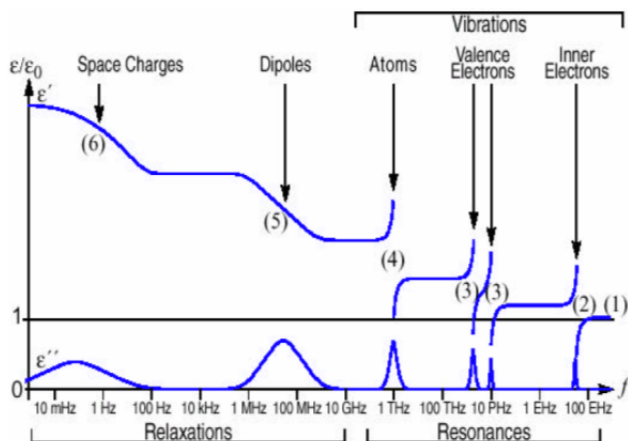


Fig.1. The different effects on the permittivity and dielectric losses of relaxation and resonance modes

Fig.1. shows that each type of polarization induces a decrease in the permittivity with frequency as well as a peak of dielectric losses. This interweaving between the real permittivity and the dielectric losses is described by the relations of Kramers-Kronig.

Classically, four relaxation functions have been developed and widely applied to describe dielectric relaxation: Debye [10], Cole-Cole [11], Davidson-Cole [12], and Havriliak-Negami [13] functions. Out of these four, the HN function is the most general because of its ability to model a broad and asymmetric distribution of relaxation times and it is employed in the following analysis.

Dispersion in small organic or inorganic molecules is studied in measuring the complex dielectric constant of the material at constant temperature on the wider range of frequencies than possible. The temperature is then varied and the repeated measurements until the desired temperature range are covered. From of each isothermal data set the Cole-Cole diagrams are obtained and analyzed to check whether a semicircular arc is obtained in accordance with the equation Cole-Cole or a faulty bow in accordance with the Davidson-Cole equation is obtained. The Cole-Cole diagrams of polymers obtained by isothermal measurements do not lend themselves to the simple processing that is used in the case of simple molecules. The main reasons for this difficulty are:

- The dispersion in polymers is usually very wide so that fixed temperature data are not sufficient for a dispersion analysis. Data from several temperatures should be pooled to describe dispersions in a meaningful way.

- The shapes of Cole-Cole diagrams are rarely as simple as those obtained with molecules of simpler structure making the determination of the very uncertain dispersion parameters.

In an attempt to study the -dispersion in many polymers, Havriliak and Negami measured the dielectric properties of several polymers. -dispersion in a polymer is the process

associated with the glass transition temperature, where many changes in the physical properties are significant. In several polymers the Cole-Cole diagram is linear at high frequency and an arc of a circle in the low frequencies. Attempts to adjust to an arc (Cole-Cole) is possible at lower frequencies but not at higher frequencies. Similarly, an attempt to fit with an oblique arc (Cole-Davidson) is possible at higher frequencies, but not at lower frequencies. Havriliak and Negami (HN) proposed to the complex dielectric constant the following equation:

$$(1) \quad \varepsilon^*(\omega) = \varepsilon_\infty + \frac{\varepsilon_s - \varepsilon_\infty}{\left\{1 + (i\omega\tau_{HN})^{(1-\alpha)}\right\}^\beta}$$

It is easily seen that this equation is both a generalization of the Cole-Cole equation, to which it reduces for  $\beta=1$ , and a generalization of the Cole-Davidson equation to which it reduces for  $\alpha=0$ . Separation of the real and the imaginary parts gives rather intricate expressions for  $\varepsilon'$  and  $\varepsilon''$  can be related to the zero frequency  $\varepsilon_s$  and infinite frequency  $\varepsilon_\infty$  limits.

$0 \leq \alpha < 1$  represents the width of the distribution.  $0 < \beta \leq 1$  represents the skewness distribution.

This function is a generalization of the three previous ones:

$\alpha = 0$  and  $\beta = 1$ , Debye's equation;

$\alpha \neq 0$  and  $\beta = 1$ , Cole-Cole's equation;

$\alpha = 0$  and  $\beta \neq 1$ , Cole-Davidson's equation.

The separation of the real and imaginary parts gives rather complex expressions

for  $\varepsilon'$  and  $\varepsilon''$

$$(2) \quad \varepsilon'(\omega) = \varepsilon_\infty + \frac{\cos(\beta\varphi)}{\left\{1 + 2(\omega\tau_0)^{(1-\alpha)} \sin\left(\frac{1}{2}\alpha\pi\right) + (\omega\tau_0)^{2(1-\alpha)}\right\}^{\frac{\beta}{2}}}$$

$$(3) \quad \varepsilon''(\omega) = (\varepsilon_s - \varepsilon_\infty) + \frac{\sin(\beta\varphi)}{\left\{1 + 2(\omega\tau_0)^{(1-\alpha)} \sin\left(\frac{1}{2}\alpha\pi\right) + (\omega\tau_0)^{2(1-\alpha)}\right\}^{\frac{\beta}{2}}}$$

$$(4) \quad \varphi = \arctan \left[ \frac{(\omega\tau_0)^{(1-\alpha)} \cos\left(\frac{1}{2}\pi\alpha\right)}{1 + (\omega\tau_0)^{(1-\alpha)} \sin\left(\frac{1}{2}\pi\alpha\right)} \right]$$

These models were simulated in the frequency domain in order to identify each behavior. These results are presented for the real permittivity  $\varepsilon'$ , the dielectrics losses  $\varepsilon''$  in Fig. 2. and  $\tan(\delta)$  in Fig.3 [14].

We therefore find that the frequency of the peak of  $\tan(\delta)$  depends both on  $t$ , but also  $\varepsilon_\infty$  and  $\varepsilon_s$ . For the other models, the frequency of the peak depends on the same parameters, with in addition the coefficients  $\alpha$  and  $\beta$ .

Thus any reasoning on the frequency of the relaxation peak visible on the  $\tan(\delta)$  should be done with the utmost caution. In particular, extract activation energy on the peak of  $\tan(\delta)$  to deduce that of the relaxation phenomenon can be done if and only if the  $\varepsilon_\infty$ ,  $\varepsilon_s$ ,  $\alpha$  and  $\beta$  parameters remain constant regardless of the temperature.

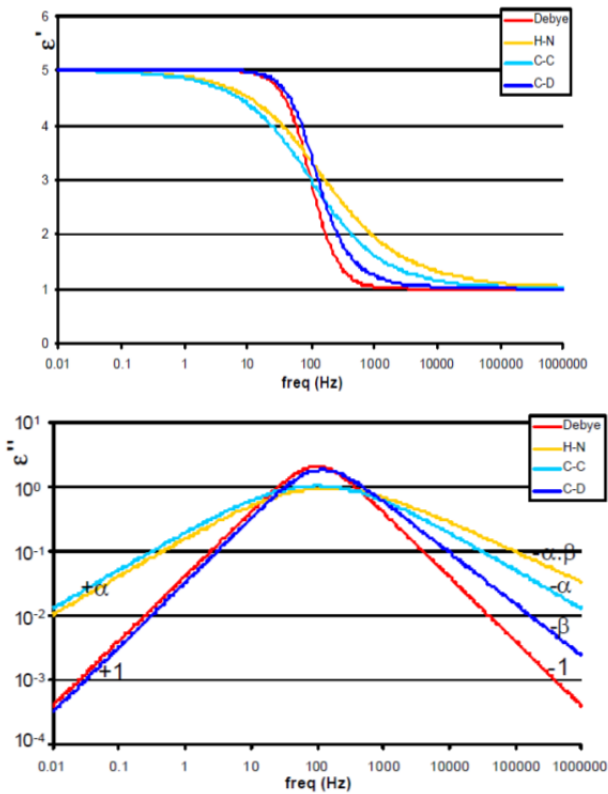


Fig. 2. Variation of real permittivity and dielectric losses as a function of the frequency for different models. ( $\epsilon_{\infty} = 1$ ,  $\epsilon_s = 5$ ,  $\tau = 10^{-2} / (2 \pi)$  in seconds  $\alpha = 0.6$  and  $\beta = 0.8$ ).

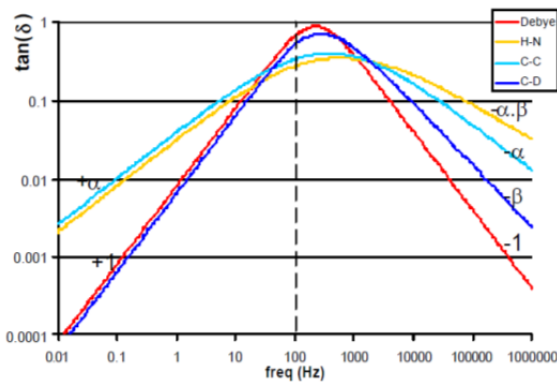


Fig.3. Variation of the tangent of the loss angle as a function of the frequency for different models. ( $\epsilon_{\infty} = 1$ ,  $\epsilon_s = 5$ ,  $\tau = 10^{-2} / (2 \pi)$  in seconds  $\alpha = 0.6$  and  $\beta = 0.8$ ).

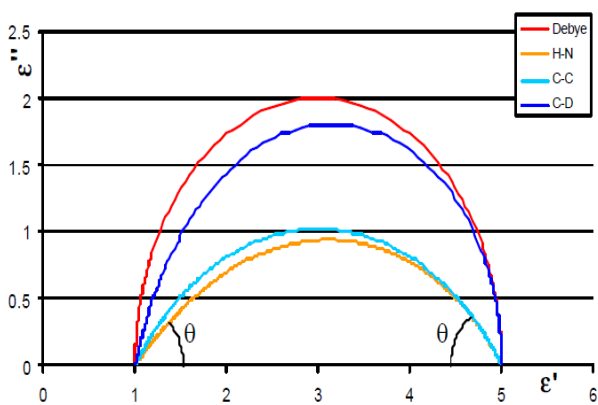


Fig.4. The Cole-Cole graph the dielectric losses as a function of the real permittivity for the different models ( $\epsilon_{\infty} = 1$ ,  $\epsilon_s = 5$ ,  $\tau = 10^{-2} / (2 \pi)$  in seconds  $\alpha = 0.6$  and  $\beta = 0.8$ ).

Fig.4. represents the Cole-Cole graph which gives the dielectric losses as a function of the real permittivity for the models presented previously

### Research Method

Let the constant field  $E_0$ , at time  $t=0$ , applied to a dielectric, the resulting electrical displacement  $D(t)$  at any later time is given by :

$$(5) \quad D(t) = \epsilon_0 [\epsilon_{\infty} + (\epsilon_s - \epsilon_{\infty})\phi(t)]E_0$$

$\phi(t)$  describing the evolution over time of the underlying orientation process and verify  $\phi(t)$  and  $\phi(\infty) = 1$ . We further assume that the rates at which the rise of the dipole polarization  $P_d(t)$  towards its equilibrium value  $P_d(\infty) = \epsilon_0 (\epsilon_s - \epsilon_{\infty})E_0$  is proportional to its initial equilibrium value :

$$(6) \quad \dot{P}_d(t) = - \frac{P_d(\infty) - P_d(t)}{\tau}$$

$\tau$  is a characteristic time constant, it is the "dielectric relaxation time", it refers to a gradient of a stress (the resulting polarization or electrical displacement) following a sudden change in a stress (the applied electric field).

When a macroscopic relaxation function obeys a simple exponential law:[10].

$$(7) \quad \phi(t) = e^{-\frac{t}{\tau}}$$

Debye's well-known formula for the function of frequency-dependent dielectric permittivity is given by :

$$(8) \quad \frac{\epsilon^*(\omega) - \epsilon_{\infty}}{(\epsilon_s - \epsilon_{\infty})} = \frac{1}{1 + i\omega\tau}$$

Experimental data are best described by exponential relaxation laws. This requires empirical relationships, which take into account the distribution of relaxation times. In the most general sense, the non-Debye dielectric behavior can be described in terms of a continuous relaxation time distribution  $\Phi(\tau)$ , this implies that the complex dielectric permittivity can be presented as follows:

$$(9) \quad \frac{\epsilon^*(\omega) - \epsilon_{\infty}}{\epsilon_s - \epsilon_{\infty}} = \int_0^{\infty} \frac{\Phi(\tau)}{1 + i\omega\tau} d\tau$$

where the distribution function  $\Phi(\tau)$  satisfies the standardization requirement :

$$(10) \quad \int_0^{\infty} \Phi(\tau) d\tau = 1$$

The corresponding expression for the decay function is :

$$(11) \quad \phi(t) = \int_0^{\infty} \Phi(\tau) e^{-\frac{t}{\tau}} d\tau$$

By virtue of relation (11) it must be clearly understood that the calculation of  $\Phi(\tau)$  does not, in itself, provide anything more than another way of describing the dynamic behavior of dielectric materials in the time domain. Moreover, such a calculation is a mathematically poorly posed problem, which leads to other difficulties of a mathematical nature. This difficulty may be one of the reasons why the superposition of some parametric functions has been privileged in the description of dielectric response spectra [15]

Diffusive representation (DR) is an approach dedicated to the analysis, approximation and synthesis of integral non-rational operators of pseudo-differential type. This method is used in many problems in modeling, numerical simulation, estimation and control. For linear systems, the Laplace transformation is a basic tool, allowing to transform a constant coefficient differential equation into an algebraic equation that can be solved with relatively few calculations.

However, even in the linear case, the classical frequency approach is not suitable for real-time problems (identification, tracking, control, etc.).[16]. For non-linear systems, many approaches have been used to solve various problems in a satisfactory and inexpensive way [17]. Among these approaches, diffusive representation (DR) introduced in 1998 by G. Montseny, is an approach of general scope that extends to various fields: analysis of dynamic systems, modeling and synthesis of signals and images, modeling and identification of physical processes, robust control, control of distributed systems, etc. Several examples of the use of DR are introduced in electrical engineering, diffusive control of an electric machine; [18], FPGA implementation of diffusive realization for a distributed control operator[19], identification of the dynamics of a lead-acid battery by a diffusive model [16], taking into account the distribution of relaxation times in dielectric materials, taking into account the eddy currents in a winding [20], diffusive representation modelling thermal and overvoltage for permanent magnet synchronous motor fed by voltage inverter[21] and identification of non-linear dynamic models for physical systems such as Micro-Electro-Mechanical Systems (MEMS) from measurement data, presented in [22].

The concept of diffusive representation (DR) introduced in order to transform certain non-standard causal convolutional operators such as fractional order integrations or derivations into dissipative input/output linear dynamic systems in a functional state space.

The D.R. allows formalism adapted to a dynamic analysis of the input/output type of pseudo-differential operators (of a non-rational nature) in the form of symbol  $\eta(\xi, t)$

$$(12) \quad H(t, p) = \int_0^{+\infty} \frac{\eta(\xi, t)}{p + \xi} d\xi$$

The symbol  $\eta(\xi, t)$  is obtained by the inverse Laplace transform of the inverse response  $h(t)$ :

$\eta(\xi, t) \xrightarrow{\mathcal{L}_\xi} h(t, s) \xrightarrow{\mathcal{L}_s} H(t, p)$  The symbol  $\eta(\xi, t)$  when it exists, fully characterizes the operator and must be considered as the usable symbol.

The input-output relation is expressed in the form of an equation in infinite dimension called diffusive realization.

$$(13) \quad \begin{cases} \partial_t \Psi(\xi, t) = -\xi \Psi(\xi, t) + u(t), & \Psi(\xi, 0) = 0 \\ y(t) = \int_0^{+\infty} \eta(t, \xi) \Psi(\xi, t) d\xi \end{cases}$$

Numerical simulation, in addition to temporal discretization, requires a discretization of the symbol according to the variable  $\xi$ .

We are looking for an approximation of the diffusive realization of an H operator ( $\partial t$ ). To do this, we give ourselves a discretization  $\{\xi_k\}_{k=1:K}$  of  $\xi$  from which we can, in various ways, define a continuous time model of finite dimension, making it possible to realize an operator approximated to  $H(\partial t)$ . The range covered is fixed by the extreme values  $\xi_1$  and  $\xi_K$ . This range will depend on the dynamics of the operator that we wish to approximate by a realization of a state of dimension [15].

This choice allows, in a logarithmic representation, to assign the same importance to each of the studied decades, but this choice is however not necessary from a mathematical point of view and one can take for example an arithmetic distribution of  $\xi_k$  in some cases [15].

The low frequencies having more "weight" than the high frequencies in the realization of the operator, a discretization in  $\xi$  all the less fine as the frequencies are large will be used. The points of discretization  $\xi_k$  are thus

often defined as elements of a geometrical sequence of reason  $r$  :

$$(14) \quad \{\xi\}_{k+1} = r\{\xi\}_k$$

to cover the frequency band  $[\xi_1, \xi_K]$ .

The approximate diffusive realization of the corresponding K-dimension is written[12] :

$$(15) \quad \begin{cases} \partial_t \psi_k(t) = -\xi_k \psi_k(t) + u(t), & \psi_k(0) = 0, \quad k = 1:K \\ y(t) = \sum_{k=1}^K \eta_k \psi_k(t) \end{cases}$$

Thus writing the model in an approximate form of a classical equation of state leads to:

$$(16) \quad \begin{cases} \frac{\partial \psi(t)}{\partial t} = A\psi(t) + Bu(t), & \psi(0) = 0, \\ y(t) = C\psi(t), \end{cases}$$

With  $\psi(t) = (C\psi_1(t), \dots, C\psi_K(t))^T$ ,  $A = \text{diag}(\xi_k)$ ,

$$B = (1, \dots, 1)^T \text{ et } C = (\eta_1, \dots, \eta_K).$$

To obtain directly an approximation of  $H(\partial/\partial t)$ , i.e. to solve a particular optimization problem, let's take a column vector  $\bar{H} = (\bar{H}(j\omega)_m)_{m=1:M}$  frequency response measurement of  $H(\partial/\partial t)$ .

We can define the column vector :

$$(17) \quad H_K = \left( \sum_{k=1}^K \frac{\eta_k}{j\omega_m + \xi_k} \right)$$

in which the column vector  $\eta := (\eta_k)_{k=1:K}$  must be found. The vector  $H_K$  can be written in condensed form

$$(18) \quad H_K = G\eta$$

With  $G := [G_{(m,k)}]$  an  $M \times K$  matrix, defined by:

$$(19) \quad G_{m,k} = \frac{1}{j\omega_m + \xi_k}$$

The problem is to look for a vector  $\eta$  that minimizes the Euclidean distance between the two vectors. The problem is to look for a vector  $\eta$  that minimizes the Euclidean distance between the two vectors  $\bar{H}$  and  $H_K$  [17]:

$$(20) \quad \min_{\eta \in \mathbb{R}^K} \|(G\eta)_m - \bar{H}\|^2$$

This leads to a unique solution  $\eta$  given by:

$$(21) \quad \hat{\eta} = [\text{Re}(G^*G)]^{-1} \text{Re}(G^*\bar{H})$$

with  $G^*$  dual matrix of  $G$  and  $\bar{H} := (H_m)_{m=1:M}$

In practice, only a finite set of data is accessible, for example for a frequency grid.  $\{\omega_m\}_{m=1:M}$  The transfer function identified  $\tilde{H}$  is then given by:

$$(22) \quad \tilde{H}(j\omega) = \sum_{k=1}^K \frac{\hat{\eta}_k}{j\omega + \xi_k}$$

The approximate optimal state realization of dimension K of the unknown operator  $H(\partial/\partial t)$  obtained from the vector of frequency measurements  $\bar{\eta}$  is :

$$(23) \quad \begin{cases} \frac{d\psi_k}{dt} = -\xi_k \psi_k + u, & \psi_k(0) = 0, \quad k = 1:K, \\ y(t) = \sum_{k=1}^K \hat{\eta}_k \psi_k(t) \end{cases}$$

The obtained solution is in general sensitive to measurement noise when the matrix  $G$  is ill-conditioned, especially in the case where  $\xi_1 \ll \xi_K$  when we want to cover several decades. we use the Tikhonov regularization method, the optimization problem (20) becomes:

$$(24) \quad \min_{\eta} \{\|G\eta - \bar{H}\|^2 + \varepsilon\|\eta\|^2\}$$



This is written in a finite dimension:

$$(25) \quad \min_{\eta} \{ \sum_{m=1}^M |[(G\eta)_m - \bar{\eta}_m]^2 + \varepsilon \|\eta\|^2 \}$$

and the solution is :

$$(26) \quad \hat{\eta} = [Re(G^*G) + \varepsilon \|\mathbb{I}\|^{-1} ReG^* \bar{\eta}]$$

The error increases at the boundaries of the domain of the selected  $\xi_k$ , it is a problem related to the discretization of the  $\xi$  on the range  $[1, M]$ . To limit the side effects on the identified solution, one must choose  $\xi_k$  over a range  $[\xi_1, \xi_K]$  included in  $[1, M]$  [18]

This involves determining the diffusive symbol using system time response measurements. Given a time interval  $t \in [0, T]$  over which the input  $u(t)$  of the system is known and the measured output is noisy,

$$(27) \quad \bar{y}(t) = y(t) + e(t)$$

Let the linear operator :

$$(28) \quad \begin{aligned} \frac{\partial \psi(t)}{\partial t} &= A\psi(t) + Bu(t), \quad \psi(0) = 0, \\ y(t) &= C\psi(t), \end{aligned}$$

with  $\Psi$  solution of the dynamic equation in infinite dimension

$$(29) \quad \frac{\partial \Psi(t, \xi)}{\partial t} = -\xi \Psi(t, \xi) + u(t), \quad \Psi(0, \xi) = 0, \quad \xi > 0$$

or

$$(30) \quad \Psi(t, \xi) = \int_0^t e^{-\xi(t-s)} u(s) ds$$

The solution of  $y^- = G\eta$ , obtained from

$$(31) \quad \min_{\eta} \|G\eta - \bar{y}\|^2,$$

is of the same structure as that obtained from the frequency response

$$(32) \quad \hat{\eta} = (G^*G)^{-1}(G^*\bar{y}),$$

In order to obtain a finite formulation we discretize  $\xi$  and  $t$  such that :

$$(33) \quad \hat{\eta}(\xi) = \sum_{k=1}^K \eta_k \delta(\xi - \xi_k)$$

and  $t$  on  $[0, T]$  according to the vector  $[t_m]_{m=1:M}$ , it notes

$$(34) \quad \begin{aligned} \bar{y}_m &= \bar{y}(t_m), \quad G_{m,k} = \Psi(t_m, \xi_k) \\ &= \int_0^{t_m} e^{-\xi_k(t_m-\tau)} u(\tau) d\tau \end{aligned}$$

Considering the vector  $\eta = [\eta_k]_{k=1:K \in \mathbb{R}^K}$  and the matrix  $G = [G_{m,k}]$ , problem (27) is transformed into a finite dimension :

$$(35) \quad \min_{\eta \in \mathbb{R}^K} \sum_{m=1}^M |(G\eta)_m - \bar{y}_m|^2$$

the solution can be written:

$$(36) \quad \hat{\eta} = (G^T G)^{-1}(G^* \bar{y})$$

with  $\bar{y}$  the vector  $[y_m]_{m=1:M}$  and regularization by Tikhonov's method gives :

$$(37) \quad \hat{\eta} = (G^T G + \varepsilon \mathbb{I})^{-1}(G^* \bar{y})$$

#### Algorithm: identification under DR

1. initialization of variables ( $M, K, f_{max}, f_{min}$ ) ;
2. calculation of  $r$  ;
3. reading data from an Excel file ;
4. choice of vector  $[\omega_m]_{m=1:M}$  ;
5. calculation of  $\mathbb{H}(j\omega_m) = \sum_{k=1}^K \frac{\eta_k}{j\omega_m + \xi_k}$  ;
6. choice of vector  $[\xi_k]_{k=1:K}$  following  $r$  ;
7. construction of the matrix  $A_{m,k} = \frac{1}{j\omega_m + \xi_k}$  ;
8. conditioning with the function  $\Lambda$  ;
9. realization of the estimated symbol  $\hat{\eta}$  by pseudo-inversion ;
10. calculation of the matrices  $A, B, C, D$  of the state model ;
11. diffusive realization of the entrance  $\eta$  ;
12. displaying results.

This algorithm is for resolution of the diffusive system, to perform the frequency identification of  $H$ , we must first choose a vector of  $[\omega_m]_{m=1:M}$  for which we obtain the frequency measurements  $\mathbb{H}(j\omega_m)$ . We then choose a vector of  $\xi_k$ , construct the matrix  $A_{m,k}$  and carry out the inversion calculation with penalization. The solution is then the vector minimizing the error between the frequency measurements and the model built from  $\xi_k$ .

#### Effect of the number of measurements ( $K$ )

The main difficulty lies in the choice of the value of  $K$  making identification delicate. From a mathematical point of view, the choice of  $K$ , the number of points  $\xi_k$  of the mesh  $[\xi_{min}, \xi_{max}]$ , is random, but for numerical reasons, this choice is important, Fig 5 and 6 show these effects.

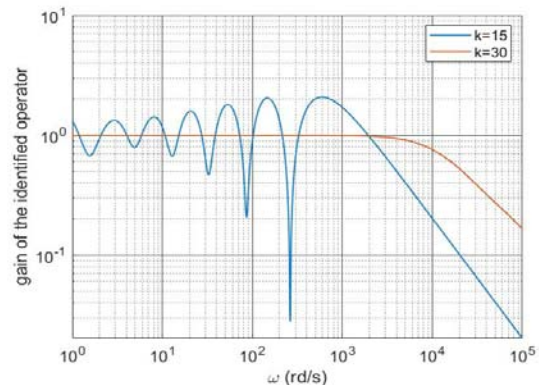


Fig.5. the gain of the identified operator we notice the oscillation of the system for  $K = 15$  and its stability for  $K = 30$ .

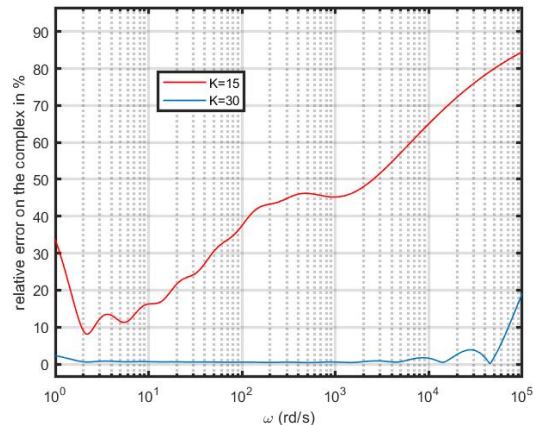


Fig.6. The relative error between the operator realized and the same operator identified by diffusive realization, we notice the effect of the choice of the number  $K$  on the relative and an energy  $Q$ .

For  $k = 30$  the stability of the system and the relative error on the identified curve does not exceed 20%. On the other hand, for  $k = 15$ , oscillations are observed on the identified curve and the relative error can reach 90%.

### Simulation Results

To realize the frequency identification of  $H$  we have chosen the vector  $[\omega_m]_{m=1:64}$ , which contains the frequency measurements  $H(j\omega_m)$ .

The discretization of the frequency axis according to the variable  $\xi$  has done in such a way that we obtain the vector  $\{\xi_k\}_{k=1:K}$  included in the interval  $[10^0, 10^5]$  in order to avoid the border effect, for  $K = 25$  we will have a vector  $\{\xi_k\}$  of 25 values distributed according to the geometric progression  $\xi_{k+1} = 1.4918\xi_k$ , with  $\xi_1 = 101$  and  $\xi_{25} = 99990$  as border values which allows us to obtain the solutions on Figure 3.

We have applied this method (RD) on a Cole-Cole model which its transfer function is given by the relation:

$$\varepsilon(p) = \frac{1}{1 + (\tau p)^\alpha}$$

PVAc) material (data:

$$\varepsilon_\infty = 3.13, \Delta\varepsilon = 6.00, f_{\max} = 10^4 \text{ Hz}, f_{\min} = 0.1 \text{ Hz}$$

$$\alpha = \{0.2, 0.4, 0.6, 0.8, 1\}$$

We were able to draw the curves of the (Fig.7) concerning the real and imaginary components of the PVAc permittivity as well as the Cole-Cole diagram.

### Interpretation and Discussion

It can be seen in (Fig.7) that there is a good superposition of the two curves, identified and simulated, except near the two borders of the frequency interval, we notice a small but important error due to the:

- Effect of the value of  $k$ , the discretization factor of  $\xi$ ; [14]
- The material of the electrodes used in the experiment [4].

The simulation program has executed for 81.2 seconds, which is relatively long, and this is due to:

- Complexity of the diffusive symbol of the Cole-Cole (C-C) model transfer
- Optimization algorithm in need of improvement.

Despite the apparent long duration of the simulation time, it remains much smaller than the durations obtained with other finite element based or other methods.

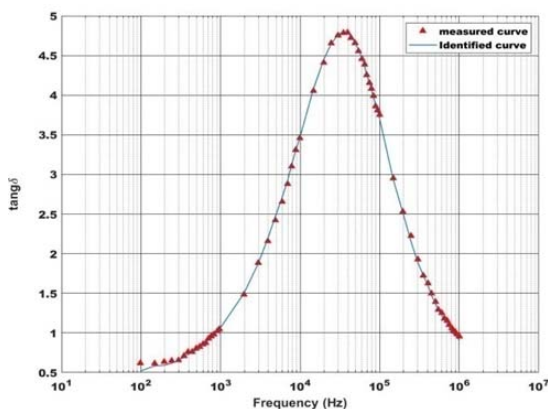


Fig.7. The measured curve ( $\Delta$ ) and the one identified by RD of the diffusive symbol of the C-C model.

The calculation of the relative error has given in the (Fig. 8), where the edge effect has clearly observed in the low frequency and high frequency regions.

In figures 9 and 10 we obtained the real and imaginary curves of the model C-C, and in (Fig.11) we represent the Cole-Cole diagram of material.

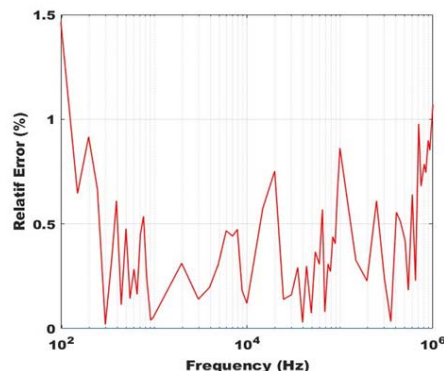


Fig.8. The relative error on the identified curve compared to the measured curve in (%).

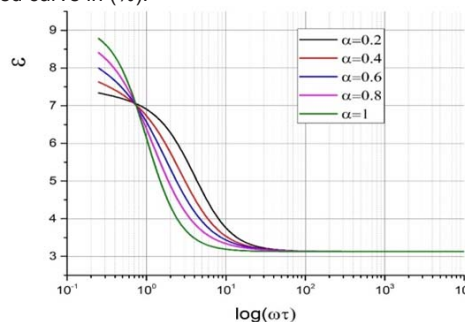


Fig.9. The Cole-Cole function: real component of the relative permittivity plotted against log (frequency) for several values of the broadening parameter ( $\alpha$ ).

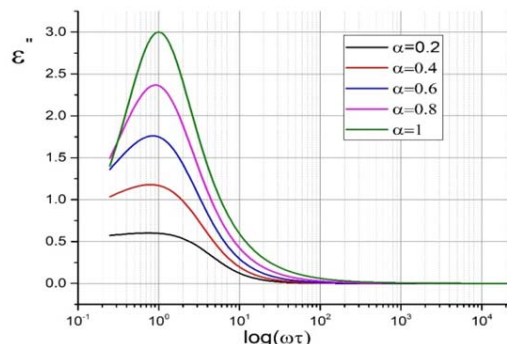


Fig.10. The Cole-Cole function: imaginary component of the relative permittivity plotted against log (frequency) for several values of the broadening parameter ( $\alpha$ ).

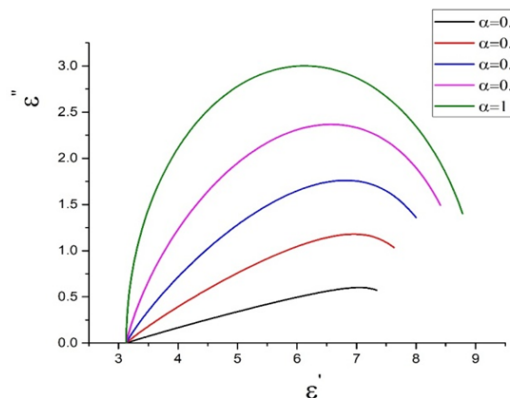


Fig.11. Complex plane plot of the Cole-Cole function for various values of the broadening parameter ( $\alpha$ ).

## Conclusion

In this work, we have presented the different main relaxation models adapted nowadays for the analysis of dielectric relaxation spectrum and mainly the C-C model that we have used afterwards. An analysis of the so-called diffusive representation tool is necessary to present the mathematical aspects of this tool and a good understanding of its foundations. We presented the application of this new method to the identification of dielectric relaxation of the C-C model. In perspective, it has recommended to implement this method in an FPGA, in order to increase its speed further.

## Acknowledgments

This work has financially supported by Directorate General for Scientific Research and Technological Development (DGRST) Ministry of Higher Education and Scientific Research Algeria, under the Scientific Program /PRFU. Contract /, No A01L07UN030120180002

**Authors** PhD student Yahia Saadaoui, Laboratoire d'études et développement des matériaux semi-conducteurs et diélectriques (LeDMaScD), Amar Telidji University of Laghouat, Ghardaia road, Laghouat 03000, Algeria, E-mail: [y.saadaoui@cu-aflou.edu.dz](mailto:y.saadaoui@cu-aflou.edu.dz), prof dr Boubakeur Zegnini, Laboratoire d'études et développement des matériaux semi-conducteurs et diélectriques (LeDMaScD), Amar Telidji University of Laghouat, PoBox 37 G, Mkam Laghouat 03000, Algeria, E-mail: [b.zegnini@lagh-univ.dz](mailto:b.zegnini@lagh-univ.dz), prof dr Seghier Tahar, Laboratoire d'études et développement des matériaux semi-conducteurs et diélectriques (LeDMaScD), Amar Telidji University of Laghouat, PoBox 37 G, Mkam Laghouat 03000, Algeria, E-mail: [t.seghier@lagh-univ.dz](mailto:t.seghier@lagh-univ.dz).

## REFERENCES

- [1] T.Raïssi et al., Analyse de spectres de relaxation diélectrique par inversion ensembliste : une première approche, Revue Internationale de Génie Electrique, CERTES, Université Paris XII, 2005.
- [2] A.A. Lukichev, Graphical method for the Debye-like relaxation spectra analysis, J. Non-Cryst. Solids (2011), doi:10.1016/j.jnoncrsol.2011.10.022
- [3] T.Blythe, D.Bloor, Electrical Properties of Polymers, second edition, Cambridge University Press, 2005.
- [4] G.G.Raju, Dielectrics in Electric fields, Marcel Dekker, Inc, New York, 2003.
- [5] I.J.Lopez and al., Relaxation processes in polymers filled with nanoparticles, Journal of Non-Crystalline Solids 356 (2010) 574–577.
- [6] N.D.Hoang, Etude des Propriétés Électriques des Élastomères Silicones Utilisés pour l'Isolation Électrique, thèse de doctorat, Université Joseph Fourier Grenoble 1, Novembre 2005.
- [7] M.Ambid, Evaluation de Nanocomposites Polypropylène/Silicate pour l'isolation électrique : Etude des Phénomènes de Polarisation, de Conduction et des Propriétés Optiques, thèse de doctorat, Université de Toulouse, Mai 2007.
- [8] J.C.Dubis, Propriétés Diélectriques des Polymères, techniques de l'ingénieur, E 1 850.
- [9] C.Menguy, Mesure des Caractéristiques des Matériaux Isolants Solides, techniques de l'ingénieur, D 2 310.
- [10] D.W. Davidson, R.H. Cole. Dielectric relaxation in glycerol, propylene glycol, and normalpropanol. J. Chem. Phys., 19, pp. 1484–1490. 1951,
- [11] S. Havriliá, S. Negami. A complex plane representation of dielectric and mechanical relaxation processes in some polymers. Polymer, 8 p. 161.,1967,
- [12] Y.N. Huang, C.J. Wang, E. Riande. Superdipole liquid scenario for the dielectric primary relaxation in supercooled polar liquids. J. Chem. Phys., 122,2005.
- [13] M. Wubbenhorst, J. van Turnhout. Analysis of complex dielectric spectra. I. Onedimensional derivative techniques and three-dimensional modelling. J. Non-Cryst. Solids, 305, pp. 40–49,2002.
- [14] Jean-Philippe Manceau, Etude du phénomène de relaxation diélectrique dans les capacités Métal-Isolant-Métal, Thèse de doctorat, Université Grenoble 1, Joseph Fourier, France, 2008
- [15] C.Casenave, Représentation Diffusive et Inversion Opératoireielle pour l'Analyse et la Résolution de Problèmes Dynamiques non Locaux, thèse de doctorat, Université de Toulouse, Décembre 2009.
- [16] F.Monteghettia, D.Matignonb, E.Piota et L.Pascala, Simulation temporelle d'un modèle d'impédance de liner en utilisant la représentation diffusive d'opérateurs, 13e Congrès Français d'Acoustique, 11 April 2016 - 15 April 2016 (Le Mans, France).
- [17] L. Laudebat, P. Bidan, and G. Montseny. Modeling and optimal identification of pseudodiffere ntial electrical dynamics by means of diffusive representation i. modeling. IEEE Transaction on Circuits and System I, 51 :1801–1813, 2004.
- [18] A.Rumeau, Modélisation Comportementale en Génie Électrique sous Représentation diffusive : Méthodes et Applications, thèse de doctorat Université de Toulouse, Novembre 2009.
- [19] L.Laudebat, Approche des Phénomènes de Relaxation Diélectrique par Réalisation Diffusive, Laboratoire de Génie Électrique de Toulouse, Université Paule Sabatier, Juin 2003.
- [20] G.Garcia, J.bernussou, Identification of the Dynamics of a Lead Acid Battery by a Diffusive Model, ESAIM Proceedings Fractional Differential Systems Models Methods and Applications, Volume 5 87-98, 1998.
- [21] KHALED et al., Diffusive representation modelling thermal and overvoltage for permanent magnet synchronous motor fed by voltage inverter, Turk J Elec Eng & Comp Sci (2019) 27: 3951 – 3966 © TÜBİTAK, doi:10.3906/elk-1811-183
- [22] R.H. Boyd, G.D. Smith, Polymer Dynamics and Relaxation, Cambridge University Press, First published 2007.